The central projections of the laryngeal nerves in the rat

Arán Pascual-Font,[1] Ignacio Hernández-Morato,[1] Stephen McHanwell,[2] Teresa Vázquez,[1] Eva Maranillo,[1] Jose Sañudo[1] and Francisco J. Valderrama-Canales[1]

[1]*Departamento de Anatomía y Embriología Humana I, Facultad de Medicina, Universidad Complutense de Madrid, Spain*
[2]*Oral Biology, School of Dental Sciences, Newcastle University, Newcastle, UK*

Abstract

The larynx serves respiratory, protective, and phonatory functions. The motor and sensory innervation to the larynx controlling these functions is provided by the superior laryngeal nerve (SLN) and the recurrent laryngeal nerve (RLN). Classical studies state that the SLN innervates the cricothyroid muscle and provides sensory innervation to the supraglottic cavity, whereas the RLN supplies motor innervation to the remaining intrinsic laryngeal muscles and sensory innervation to the infraglottic cavity, but recent data suggest a more complex anatomical and functional organisation. The current neuroanatomical tracing study was undertaken to provide a comprehensive description of the central brainstem connections of the axons within the SLN and the RLN, including those neurons that innervate the larynx. The study has been carried out in 41 adult male Sprague–Dawley rats. The central projections of the laryngeal nerves were labelled following application of biotinylated dextran amines onto the SLN, the RLN or both. The most remarkable result of the study is that in the rat the RLN does not contain any afferent axons from the larynx, in contrast to the pattern observed in many other species including man. The RLN supplied only special visceromotor innervation to the intrinsic muscles of the larynx from motoneurons in the nucleus ambiguus (Amb). All the afferent axons innervating the larynx are contained within the SLN, and reach the nucleus of the solitary tract. The SLN also contained secretomotor efferents originating from motoneurons in the dorsal motor nucleus of the vagus, and special visceral efferent fibres from the Amb. In conclusion, the present study shows that in the rat the innervation of the larynx differs in significant ways from that described in other species.

Key words: dorsal motor nucleus of vagus; larynx; nucleus ambiguus; nucleus of the solitary tract; solitary tract.

Introduction

In humans, the larynx serves three important functions: respiratory, protective, and phonatory (Wyke & Kirchner, 1976; Sasaki, 2006; McHanwell, 2008). Thus, laryngectomy or laryngeal nerve dysfunction leads to a profound disability in the affected individual far beyond simply effects upon voice. Therapeutic approaches involving laryngeal transplantation, or laryngeal nerve reconnection, have yet to be developed routinely (Ogura et al. 1970; Crumley, 1982; Brondbo et al. 1992; Berke et al. 1993; Zheng et al. 1996). It was stated that non-selective reinnervation limits the success of transplantation, or nerve reconnection (Crumley,

2000). This, together with the obvious difficulty of analysing *in vivo* human laryngeal neuroanatomy and function, means that it is necessary to develop animal models to increase our knowledge on the mechanisms governing laryngeal re-innervation as a key factor to ensure successful laryngeal transplantation. But prior to this potential clinical application, a thorough understanding of normal laryngeal anatomy and innervation is required.

Since Galen, it is well known that the larynx is connected to the CNS by the nerves called laryngeal nerves, and it was in the 19th century that Magendie identified the nerve that innervates the cricothyroid muscle (Morrison, 1952). These branches of the vagus nerve, the superior laryngeal nerve (SLN) and the recurrent laryngeal nerve (RLN), convey the fibres of the afferent and efferent systems that control the function of the larynx (Wyke & Kirchner, 1976; Sasaki, 2006; McHanwell, 2008). It is generally accepted that the SLN innervates the cricothyroid muscle and the supraglottic mucosa, whereas the RLN supplies the remaining intrinsic laryngeal muscles and the infraglottic mucosa (Wyke & Kirchner, 1976; Moore & Dalley, 2006; Sasaki, 2006;

McHanwell, 2008). However, experiments in different species revealed that this statement may not always be applicable. So, there is physiological evidence showing that the motor innervation of the thyroarytenoid muscle can be provided via the external branch of the SLN (Nasri et al. 1997). Furthermore, the sensory innervation of an anterior infraglottic area in the cat was shown to be provided via the same SLN branch (Suzuki & Kirchner, 1968). The neural anatomy of the larynx is further complicated by the presence of a number of communications between the individual laryngeal nerves (Sañudo et al. 1999; Maranillo et al. 2003). While the precise functional significance of these physiological and anatomical facts remains unclear, it is reasonable to assume that functions commonly attributed to the laryngeal nerves may be more complex than the conventional descriptions imply and, therefore, to assume that, for any given species, the innervation of the larynx will follow the generally established pattern may be incorrect. This may have potential clinical implications (McHanwell, 2008), as well as being important when establishing animal models to investigate laryngeal innervation.

Therefore, the aim of the present work is to identify the central projections of the fibres conveyed by the SLN and the RLN in the rat, with the purpose of defining the functional character (afferent and/or efferent) and central connections of each laryngeal nerve.

Materials and methods

Animals

The research work reported herein was performed according to the regulations and laws governing the care and handling of animals in research from the European Union (86/609/EEC) and Spain (Royal Decree 223/1998), and was approved by the Complutense University of Madrid Committee of Animal Experimentation. A total of 41 adult, male Sprague–Dawley rats (*Rattus norvegicus*), 300–325 g b/w, were used in this study. Animals were maintained in the central facility of the Complutense University, and all surgical procedures were performed in the animal operating room within this facility. After surgical manipulations, animals received analgesic treatment consisting of buprenorphine (0.05 mg kg^{-1}) plus meloxicam (1 mg kg^{-1}) every 8 h for the first 2 days. Afterwards, they received ibuprofen every 8 h (2.5 mg kg^{-1}) during two further days.

Surgical procedures and nerve tracing protocol

Animals were anaesthetised, under aseptic conditions, with an intraperitoneal injection of xylazine (Rompun, Bayer, Spain; 8 mg kg^{-1}) plus ketamine (Imalgene, Merial, France; 90 mg kg^{-1}). Animals were maintained at 37 °C on a rat heating pad connected to a temperature controller throughout the surgery and in the recovery period following anaesthesia. The neck was opened ventrally with a sagittal incision, and the skin, salivary glands and infrahyoid muscles were reflected laterally with a wire retractor in order to expose the larynx and the related

vascular and neural structures (Fig. 1). Once each laryngeal nerve was identified and stripped out of its fascial sheath, it was isolated from the surrounding tissue by sliding a piece of parafilm beneath it. In order to enhance the diffusion of the dextran amine tracer inside the nerve fibres, the nerve was cut with the aid of fine scissors (Glover et al. 1986; Fritzsch, 1993). Except in five cases, the nerves were always traced on the left side. The RLN was always cut at a level corresponding to a transverse plane through the fifth or sixth tracheal rings and before the laryngeal branches had been given off. The SLN was cut prior to the division into its external and internal branches.

Recrystallised biotinylated dextran-amines (BDA; 3 or 10 kDa; Molecular Probes, OR, USA) or Texas red-conjugated dextran-amines (TRDA; 10 kDa; Molecular Probes) were deposited from the tip of a pin over the nerve's central stump, covering it entirely. Ten–fifteen minutes after application of the tracer to the nerve stump (Popov & Poo, 1992; Fritzsch, 1993; Reiner et al. 2000), the remaining dextran was aspirated, the parafilm removed, the surgical field thoroughly cleaned with saline solution, and the surgical wound closed in layers. Previously to
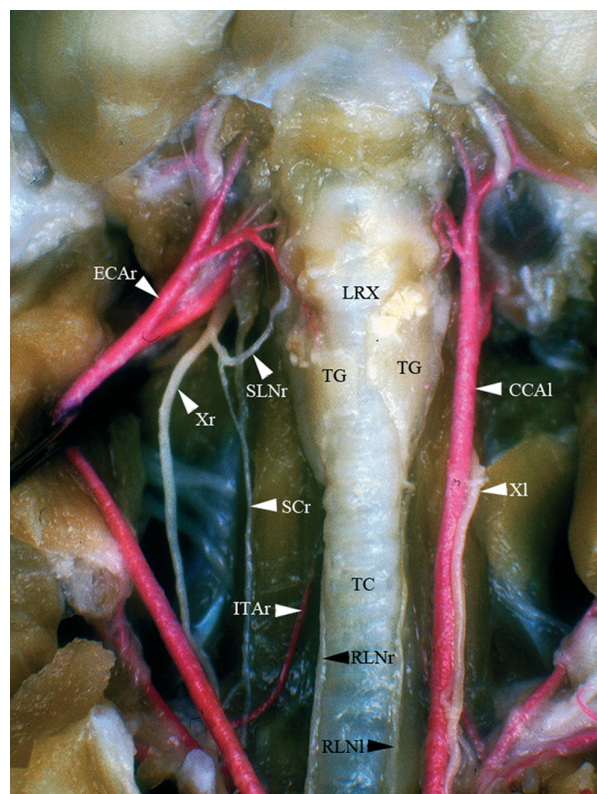

Fig. 1 Ventral dissection of the neck of the rat. The skin, salivary glands and infrahyoid muscles have been removed in order to expose the larynx, trachea, and vascular and neural structures. The right common carotid artery has been laterally rejected to allow the observation of the SLNr. Arteries have been injected through the aorta with red-stained latex. CCAl, left common carotid artery; ECAr, right external carotid artery; ITAr, right inferior thyroid artery; LRX, larynx; RLNl, left recurrent laryngeal nerve; RLNr, right recurrent laryngeal nerve; SCr, right sympathetic chain; SLNr, right superior laryngeal nerve; TC, trachea; TG, thyroid gland; Xl, left vagus nerve; Xr, right vagus nerve.

the surgery, the tip of a very sharp thin entomological pin (< 0.5 mm in diameter) was impregnated with lyophilised BDA powder and distilled water vapour was applied, this process repeated three or four times, in order to recrystallise enough tracer. In order to exclude a potential spreading of the tracer from the normal site of application to adjacent tissues, three control animals were operated, but instead of cutting the laryngeal nerves prior to the application of dextran, the laryngeal nerves were left untouched. The animals were otherwise treated as the experimental group.

Staining the labelled nerve projections

Dextrans of 10 000 MW progressed as far as 1 mm h^{-1}, and dextrans conjugated to different fluorochromes or to biotin did not show significant differences in the distances covered (Fritzsch, 1993). The mean length of the left SLN plus the left vagus was 11 mm (Maranillo E, Sañudo JR, Valderrama-Canales FJ, Vázquez T, unpublished communication), whereas the mean length of the left RLN plus the left vagus was 72 mm (Pascual-Font et al. 2006c). Thus, less than a day is required for the BDA to reach the apparent origin of the vagus via the SLN and 3 days via the RLN.

Taking into account these data, 7 days after surgery (except for a group of six rats in which the survival period was extended to 10 days), each rat was anaesthetised with a lethal intraperitoneal dose of pentobarbital (200 mg kg^{-1}) and perfused through the left ventricle with 250–300 mL of saline solution at 37 °C until the blood was removed; afterwards, 400 mL of a fixative solution containing 4% paraformaldehyde in 0.1 M phosphate buffer pH 7.4 (PB) and 10% w.v. sucrose was perfused at 4 °C. Immediately after the perfusion, the brainstems were removed from the cranium and post-fixed for 2 h in the same fixative solution, rinsed in PB, and cryoprotected by immersion overnight in 15% w.v. sucrose in PB, and then in 30% w.v. sucrose in PB until they sank. Using a freezing microtome, serial 50-μm transverse or parasagittal sections were cut and collected in 24-well plates containing PB. Depending whether the sections were to be examined by means of bright-field microscopy or fluorescent microscopy, they were processed in two different ways: for bright-field microscopy, the BDA was stained by the free-floating method using the avidin-biotin-peroxidase complex (ABC-kit; Vector, Peterborough, UK) and diaminobenzidine plus nickel as chromogen (Vector). Brainstem sections were mounted onto poly-L-lysine-coated slides, air-dried and cover-slipped following standard histological procedures. For fluorescent microscopy, the sections were stained by the free-floating method using streptavidin-conjugated fluorescein (Vector) and further processed as stated before.

Additionally, in four experimental animals (two with the SLN traced and two with the RLN traced), the ganglia of the IX and X nerves (Altschuler et al. 1989) were also extracted, fixed and 15-μm frozen sections obtained. The sections for each ganglion were processed as above described and were developed with the ABC-kit.

In those experiments where both the SLN and RLN were ipsilaterally and simultaneously labelled, BDA was applied to the SLN and TRDA to the RLN. The brainstem sections were stained with streptavidin-conjugated fluorescein (Vector) resulting in green fluorescence in those structures labelled by SLN transport in contrast to red fluorescence in the structures where the RLN projected.

All sections for fluorescent microscopy were further incubated with the nuclear stain 4′,6-diamidino-2-phenylindole dihydro-chloride (DAPI; Roche, Germany) for 15 min in order to stain nuclei fluorescent blue.

Choline acetyltransferase immunohistochemistry (ChAT-IH) combined with nerve tracing studies

In six experiments, sections from animals with TRDA-labelled SLN or RLN were subjected to an immunohistochemical protocol to detect ChAT-IH. In these cases, the surgery for nerve tracing and sample collection, fixation and sectioning was carried out as described above. Immediately after sectioning, the sections were pre-incubated with 15% normal horse serum in PB containing 0.025% Triton X-100 and 3% bovine serum albumin (1 h, 22 °C), and followed by incubation in goat anti-ChAT antibody (Chemicon, CA, USA) 1 : 100 in PB with 0.025% Triton X-100 (72 h, 4 °C). Afterwards, sections were carefully washed in PB and further incubated with biotinylated horse anti-goat antibody (Vector) 1 : 50 in PB (24 h, 4 °C). Sections were thoroughly washed in PB and then processed to the final development step with fluorescein-conjugated streptavidin (2 h, 22 °C) and nuclear fluorescent staining with DAPI. In these sections the putative cholinergic neurons will exhibit green fluorescence, the traced neurons red fluorescence, and the nuclei of all cells were fluorescent blue.

Neuron counting and positioning within the brainstem

Stained neurons were counted using either fluorescent or bright-field microscopy depending on the staining method used. In each case, the counting of the cells was undertaken by two independent observers. In each animal, the total number of labelled neurons was counted and the mean number (± SD) for each nerve group was calculated.

For counting fluorescent neurons, we developed a variant of the method described by McHanwell & Biscoe (1981a,b). The sections were examined at high magnification (40 ×) on a Nikon Eclipse 800 photomicroscope with the appropriate filter for detection of either fluorescein, Texas red or DAPI fluorescence. The following criteria were used to identify dextran-labelled fluorescent structures as a neuronal soma: the presence of a granular fluorescent product confined to the cytoplasm with a nucleus distinguishable as an area relatively clear of fluorescence; and the presence within the nucleus of a nucleolus surrounded by fluorescent reaction product. The nucleolus had to be surrounded by granular fluorescent product to exclude the possibility that it originated as a shadow from an unlabelled structure above or below the labelled structure in question. Once the neuronal perikaryon was recognised, and the nucleus was focussed, the filter was changed in order to confirm the DAPI-labelled nucleus and to identify the nucleolus (Fig. 2).

When counting neurons with bright-field microscopy, it was almost impossible to identify most of the nucleus of the BDA-filled neuronal perikarya, and no correction was made for double counting of cells. However, the perikarya were counted in each section and the total number of neurons per brainstem was compared with the data from the counts obtained from the fluorescent sections. The numerical data obtained with each method were statistically compared by means of the Student's t-test and, in all cases, the differences observed were not statistically significant. Although the theoretical prediction was that
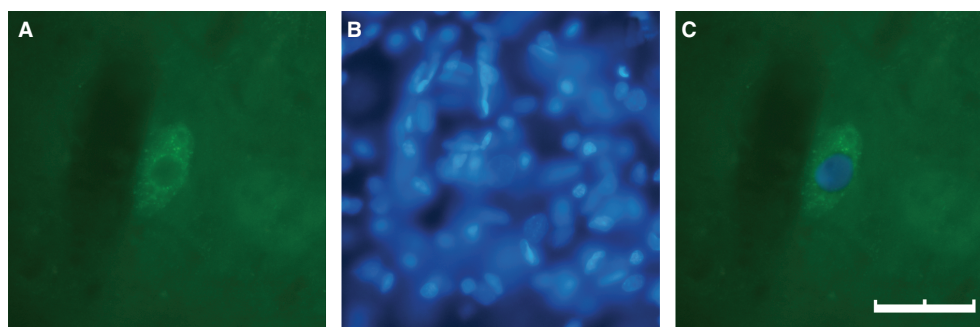
Fig. 2 Identification of fluorescent neurons. The neuronal cytoplasm has been traced with BDA through the SLN and green-stained with fluorescein-conjugated streptavidin (A), whereas the nucleus was blue-stained with DAPI also revealing the nucleolus (B). (C) The merge of (A) and (B), demonstrating that this neuronal profile has a clearly-defined reaction product that surrounds the nucleus, and that a nucleolus is clearly visible within this nucleus. Neurons meeting these criteria would be counted as labelled motoneurons (scale bar: 40 μm).

failure to correct for double counting of neurons with bright-field microscopy would result in higher numbers, experimentally this was clearly not the case, indicating that counting labelled neuronal fragments was not a significant source of error. There are two possible explanations for this: first, many fragments are not being counted because their small size renders their labelling less visible; secondly, due to the size of the neurons relative to the thickness of the section, the probability of double-counting of profiles of the same neuron in two different sections is negligible or statistically insignificant. These two factors may, of course, act in combination. However, from these considerations we do feel it appropriate that our counts be combined in this way. Thus, the results obtained both for the fluorescence and the bright-field methods were combined for further analysis.

The rostrocaudal location of the labelled neurons was measured and registered in reference to various brainstem landmarks (without correction for shrinkage). Structures close to both the dorsal surface and the midline were selected (the latter in order to minimise variance due to asymmetrical sectioning). The landmarks chosen were the caudalmost extent of the dorsal cochlear nucleus, the rostral limit of the area postrema (AP) and the obex. The obex is a gross anatomical structure usually defined as the point on the midline of the dorsal surface of the medulla oblongata that marks the caudal angle of the fourth ventricle, where the central canal opens into the rhomboid fossa. However, in the rat, the AP fills the caudal angle of the fourth ventricle, so we have considered the obex as the caudal end of the AP (Hamilton & Norgren, 1984; Paxinos & Watson, 2005). All the positional data presented in this study are expressed in micrometres and indicate a rostrocaudal measurement relative to the obex.

The abbreviations used to designate brainstem structures were defined by Paxinos & Watson (2005). The terminology related to the nucleus ambiguus (Amb) follows the topographical description made by Bieger & Hopkins (1987), and that for the nuclei of the solitary tract (Sol) employs the description by Hamilton & Norgren (1984).

Results

The labelled neurons and fibres were always found ipsilaterally to the traced nerve, with no evidence of contralateral projections. There were no qualitative or quantitative differences in the labelled structures or their distribution between the samples collected either 7 or 10 days after surgery. No differences were observed in relation to the side of operation.

SLN tracing studies

Application of BDA in the SLN, stained either for fluorescent or bright-field (Fig. 3) microscopy, resulted in labelled neurons within the Amb (Fig. 3A,B) and the dorsal motor nucleus of the vagus (10N; Fig. 3C). Occasionally, some aberrant neurons, first so called by Cajal because they were displaced from the Amb (Ramón y Cajal, 1909), were labelled (Fig. 4). After entering and crossing the medulla oblongata from lateral to medial, labelled fibres were observed in the sol (Fig. 3D) and ended in an area corresponding to the interstitial nucleus of the solitary tract (SolI; Hamilton & Norgren, 1984). In the two cases in which the X nerve ganglia were analysed, many ganglion cell bodies were labelled, with a distribution similar to that described by Altschuler et al. (1989).

The combined dextran-tracing and ChAT-IH experiments showed that the majority of dextran-traced neurons displayed ChAT-immunoreactivity. However, not all the putative cholinergic (ChAT-positive) neurons were labelled with dextran. These ChAT-positive dextran-negative neurons could be neurons whose axons were travelling to their targets via nerves other than the SLN or RLN, but the possibility that some neurons from the traced SLN and RLN remained unlabelled cannot be excluded. In some occasions, some dextran-labelled neurons within the external formation of the Amb could be observed.

RLN tracing studies

Following the application of tracers to the RLN, labelled neurons were detected only in the Amb, never in the 10N, and no fibres were observed at any location in the brainstem. In addition, no labelled ganglion cells were observed in the X nerve ganglia analysed. However, in common with
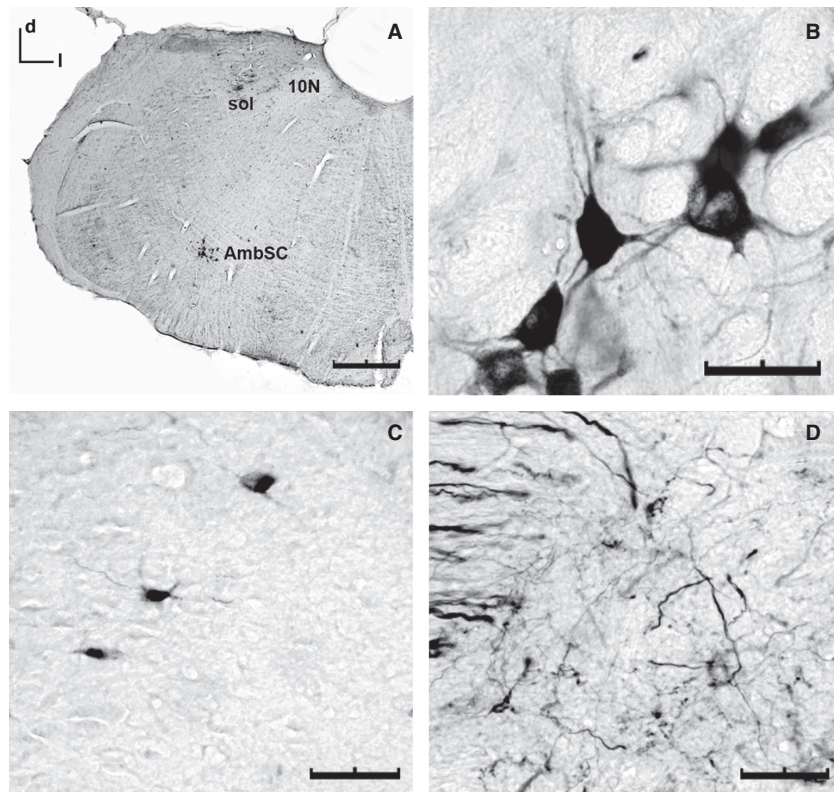
Fig. 3 Coronal sections of the medulla showing the structures labelled after the application of BDA to the ipsilateral SLN (DAB staining, bright-field microscopy). (A) Low magnification of the brainstem demonstrating labelled neurons ventrally in the AmbSC and dorsally in the 10N, as well as fibres in the sol (scale bar: 500 μm). (B and C) High magnification of neurons within the AmbSC (B) and the 10N (C) (scale bar: 50 μm). Neurons in the Amb displayed a multipolar morphology. Neurons in the 10N were smaller and fusiform. (D) Labelled axons within the sol. The thick fibres in the tract are presumed to give rise to the thinner final arborisations in the soll (scale bar: 100 μm). 10N, dorsal motor nucleus of the vagus; AmbSC, semicompact formation of the nucleus ambiguus; d, dorsal; m, medial; sol, solitary tract. All illustrations are shown in the same orientation.

some of the SLN tracing experiments, some aberrant neurons were sporadically labelled.

The results of the combined ChAT-IH and dextran-tracing experiments were similar to those found in the SLN, but no labelled neurons were found within the Amb external formation.

Ipsilateral SLN and RLN tracing studies

In order to examine the extent of overlap of sensory and motor projections of the SLN and the RLN in the brainstem, tracers were applied ipsilaterally to both nerves in eight experiments. Neurons and fibres projecting through the SLN were identified as green fluorescent-labelled structures,

while neurons and fibres projecting through the RLN were recognised as red fluorescent-labelled structures. In agreement with the tracing of a single nerve, application of tracers to the SLN resulted in labelled neurons within the Amb and the 10N, and labelled fibres reaching the Soll, whereas application of tracer to the RLN resulted in labelled neurons only in the Amb. Double-labelled structures were never observed, further increasing our confidence that tracer spread was not occurring in these experiments. In parasagittal sections, these dual nerve tracing experiments also allowed us to observe the dorsal formation column of the Amb (Bieger & Hopkins, 1987), showing that the SLN neurons are located rostrally within the semicompact formation (AmbSC) and the RLN neurons were more caudal in the
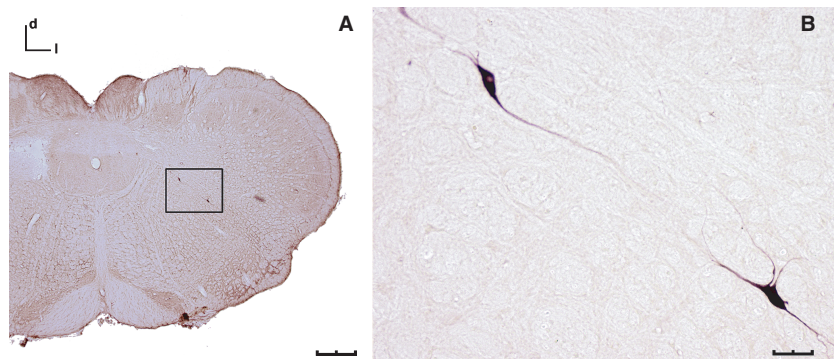

Fig. 4 Coronal sections of the medulla oblongata showing aberrant neurons labelled following the application of BDA to the SLN (DAB staining, bright-field microscopy). (A) Two aberrant neurons in an intermediate location between the Amb and the 10N (scale bar: 500 μm). (B) Enlargement of the box in (A), both aberrant neurons show fusiform morphology (scale bar: 50 μm). d, dorsal; l, lateral.

loose formation (AmbL). In transverse sections, labelled neurons from both the SLN and RLN were observed within the same section, demonstrating that there is a degree of overlap of both the AmbSC and AmbL neuronal populations (Fig. 5).

Number and location of neurons

These data are summarized in Tables 1 and 2, and Fig. 5.

Discussion

Although a number of studies on the central projections (sensory and motor) of the laryngeal nerves have been published, the current work is the first to attempt a comprehensive study. Several studies have examined either the central efferent projections of the SLN and RLN (Lawn, 1966a,b; Hinrichsen & Ryan, 1981; Pásaro et al. 1981; Schweizer et al. 1981; Yajima & Hayasi, 1983; Bieger & Hopkins, 1987; Patrickson et al. 1991a), or the central afferent projections (Patrickson et al. 1991b). Individual functional components of the SLN have also been analysed in a study by Furusawa et al. (1996). Other authors have studied only the projections of the internal branch of the SLN (Krammer et al. 1986) or, in a study of the gustatory nerves, the central origin of the SLN afferents were analysed (Hamilton &

Norgren, 1984). We have found only one work exclusively dedicated to the RLN central projections (Hisa et al. 1985). In addition to these tracing studies, many other authors have studied the central projections of the laryngeal efferent fibres by injecting horseradish peroxidase (HRP), or conjugates, into laryngeal intrinsic muscles (Gacek, 1975; Wetzel et al. 1980; Hinrichsen & Ryan, 1981; Lobera et al. 1981; Yoshida et al. 1982; Pásaro et al. 1983; Davis & Nail, 1984; Bieger & Hopkins, 1987; Portillo & Pásaro, 1988), with stereotaxic lesions in the Amb (Szentagothai, 1943), or by injecting HRP into the larynx (Kalia & Mesulam, 1980b).

Furthermore, an examination of previously published results revealed a number of inconsistencies between the findings of different authors as well as a number of yet unresolved questions. The questions that this study set out to answer were as follows. Do both laryngeal nerves contain general visceral afferent fibres? Do the neurons in the 10N known to innervate the larynx project through both laryngeal nerves? Does the larynx receive ipsilateral or bilateral innervation? And, finally, how far are the neurons of the Amb topographically segregated? Our study has attempted to address these issues by means of a neuroanatomical dextran-tracing analysis of the central projections of the adult rat laryngeal nerves and depicts a new map with the SLN containing special and general visceral efferent fibres together with general visceral afferent fibres,
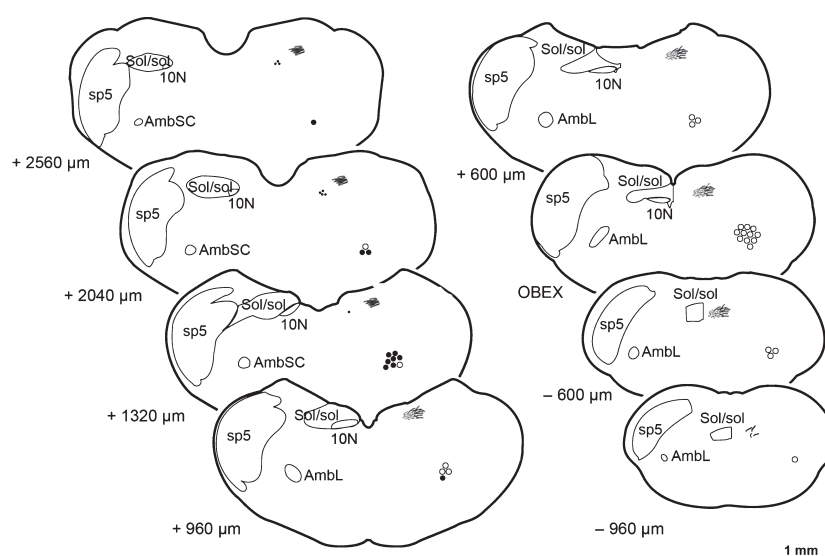

Fig. 5 Representative diagrams illustrating the distribution of the labelled neurons and fibres at eight different levels within the medulla oblongata following the application of dextran amines to the laryngeal nerves. Each diagram represents one coronal section from the medulla oblongata with the neurons and fibres shown on the right side of each diagram, while on the left side are drawn the outlines of some related nuclei and tracts as they are represented in the rat's brain atlas by Paxinos & Watson (2005). Open circles represent the motoneurons of the AmbL labelled from the RLN, whereas the solid circles represent those motoneurons labelled from the SLN within the AmbSC. The solid dots represent the neurons in the 10N, all labelled from the SLN. The lines depict the labelled fibres from the SLN, the thick ones in the sol and the thin ones representing the terminal arborisations within the Soll. Numbers on the left side of each section indicate the approximate distance in micrometres rostral (+) or caudal (−) to the obex (scale bar: 1 mm). 10N, dorsal nucleus of the vagus; AmbL, loose formation of the nucleus ambiguus; AmbSC, semicompact formation of the nucleus ambiguus; Sol∕sol, nucleus of the solitary tract and solitary tract; sp5, spinal trigeminal tract.

Table 1 Mean number (± SD) of labelled neurons in the Amb and 10N following application of tracer to either the SLN or RLN.

	Amb			10N	SoII
	Fluorescence	Bright-field	Total	Bright-field	Fluo⁄Bright
SLN	112 ± 24	122 ± 40	119 ± 36	75 ± 25	Yes
RLN	159 ± 28	152 ± 35	155 ± 30	–	No

For the Amb the table shows the number of neurons counted either with bright-field microscopy or following fluorescent labelling of the nucleus with DAPI. Both methods yield similar results and so the counts were combined to obtain the numbers shown in the 'Total' column of the table. It was not possible to employ the fluorescent-counting method for labelled neurons in 10N, and therefore only the bright-field method was employed. The table also records the presence or absence of labelled fibres in the SoII following labelling of each of the nerves.
10N, dorsal motor nucleus of the vagus nerve; Amb, nucleus ambiguus; RLN, recurrent laryngeal nerve; SLN, superior laryngeal nerve; SoII, interstitial nucleus of the solitary tract.

Table 2 Localization of labelled neurons traced from the SLN or RLN.

	Caudal-rostral location of the traced neurons (μm)		
	AmbL	AmbSC	10N
SLN	–	1230 (±150) to 2590 (±220)	1390 (±240) to 2700 (±140)
RLN	−900 (±250) to 1800 (±300)	–	–

The lengths of the columns are in micrometres (± SD) and related to the obex, thus '–' indicates caudal to the obex. Neurons traced from the SLN were found in the AmbSC and 10N, whereas neurons traced from the RLN were exclusively located in the AmbL. There was an overlapping area between the AmbL and AmbSC.
10N, dorsal motor nucleus of the vagus nerve; AmbL, loose formation of the nucleus ambiguus; AmbSC, semicompact formation of the nucleus ambiguus; RLN, recurrent laryngeal nerve; SLN, superior laryngeal nerve.

whereas the RLN only contains special visceral efferent fibres (Fig. 6). For the sake of clarity, different aspect of the current work will be discussed separately.

Technical procedures

Biotinylated dextran-amines are accurate and fast neuronal tracers capable of being transported both anterogradely and retrogradely by the axons following application onto injured nerves (Glover et al. 1986; Fritzsch, 1993; Marín & González, 1999; Reiner et al. 2000). These characteristics permit labelling of both afferent and efferent central projections within the same nerve, while reducing the risk of spurious labelling of adjacent structures by uncontrolled spread of the tracer. In order to confirm that spurious tracer spread was not a problem in our study, control experiments were performed in which dextran-amines were applied onto uninjured nerves that had simply been dissected. In

these experiments no labelled structures could be seen in the brainstem. Furthermore, labelling was always consistent between experiments so that application of tracer to the cut SLN always resulted in labelled neuronal perikarya within the Amb and the 10N, and fibres within the sol. Similarly, application of tracer to the cut RLN resulted in labelled cell bodies within the Amb, but in no other structures. Finally, in experiments in which two different tracers were applied to the SLN and the RLN on the same side, double-labelling was never observed. Thus, we feel confident that spurious spread of tracer was not a problem misleading the interpretation of our results. TRDA is a red fluorescent-conjugate of dextran amines that, in contrast to BDA, in our preliminary experiments never resulted in labelling of fibres within the sol, suggesting it was not transported anterogradely. Some authors have also observed this phenomenon (Prof. A. González, personal communication) and have confined the use of this tracer as a retrograde marker (Sánchez-Camacho et al. 2003, 2006; López et al. 2007). Consequently, we never applied TRDA to the SLN, and it was the chosen tracer for the retrograde labelling of motoneurons in the RLN in the experiments in which both laryngeal nerves were labelled simultaneously on the same side.

Central connections of the SLN afferent fibres

In the current study, labelled afferent fibres in the rat brainstem were only observed following application of tracer to the SLN and never after application onto the RLN. In a number of species, including man, it is accepted that the infraglottic cavity of the larynx receives its afferent supply from the RLN (Wyke & Kirchner, 1976; Wetzel et al. 1980; Hisa et al. 1985; Patrickson et al. 1991b; Moore & Dalley, 2006; Sasaki, 2006; McHanwell, 2008), but the few reports failing to identify afferent fibres in the RLN of the rat and the ferret (Ranson et al. 1995; Pascual-Font et al. 2006b, 2007) are supported by the current work where a lack of afferent fibres in the RLN of the rat was clearly demonstrated. There are a number of possible explanations for these contradic-
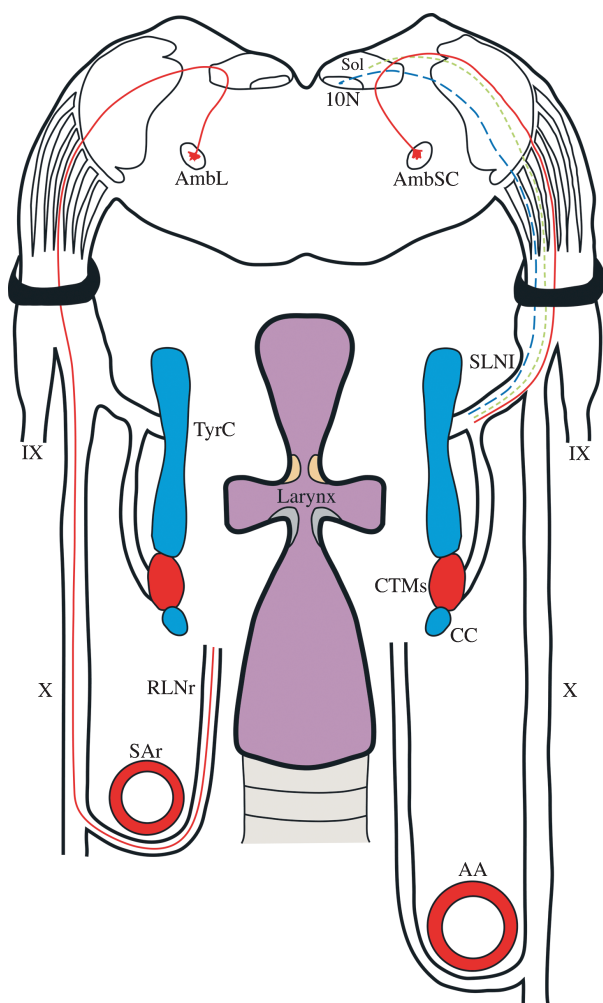
Fig. 6 Schematic drawing summarising the fibres contained in the SLN and RLN of the rat. The SLN has been represented on the right side of the picture, whereas the RLN is on the left. The SLN contains special visceral efferent fibres (red-continuous line), general visceral efferent fibres (blue-dashed line) and general visceral afferent fibres (green-dotted line). The RLN only has special visceral efferent fibres (red-continuous line). 10N, dorsal motor nucleus of the vagus; AA, aorta artery; AmbL, loose formation of the nucleus ambiguus; AmbSC, semicompact formation of the nucleus ambiguus; CC, cricoid cartilage; CTMs, cricothyroid muscle; IX, glossopharyngeal nerve; RLNr, right recurrent laryngeal nerve; SAr, right subclavian artery; SLNl, left superior laryngeal nerve; Sol, nucleus of the solitary tract; TyrC, thyroid cartilage; X, vagus nerve.

tory findings, including the possibility of spreading of tracers from the site of application, maybe to the oesophagus that lies close to the larynx and its afferent fibres also reach the SolI (Altschuler et al. 1989; Wank & Neuhuber, 2001; Neuhuber et al. 2006), the numerous connections that have been observed between laryngeal nerves (Sañudo et al. 1999; Maranillo et al. 2003), thus providing a potential route by which fibres from the infraglottic mucosa could finally travel via the SLN; furthermore, the parasympathetic

innervation to the laryngeal mucosa runs only through the SLN (see below; Hinrichsen & Ryan, 1981; Patrickson et al. 1991a; Pascual-Font et al. 2006b, 2007). Finally, electrophysiological data reported that at least some area of the infraglottic mucosa is not supplied by the RLN, as it has been demonstrated a diamond-shape region in the anterior side of the infraglottic cavity innervated by both external branches of the SLN (Suzuki & Kirchner, 1968).

We conclude that our findings represent a real species difference between rats and some other mammals, which needs to be borne in mind when carrying out experimental studies. It is curious to observe, however, that the existence of such a route by which laryngeal afferents from the infraglottic cavity reach the brainstem does not also result in some contralaterel innervation of the larynx.

This and previous reports demonstrated that the laryngeal afferents terminate in the SolI but not in other territories outside the Sol (Kalia & Mesulam, 1980a,b; Hamilton & Norgren, 1984; Altschuler et al. 1989; Saper, 2004), converging with afferent inputs also including the soft palate, pharynx (Kalia & Mesulam, 1980b; Altschuler et al. 1989), and pulmonary and tracheobronchial receptors (Kalia & Richter, 1985, 1988). Hence, SolI has been functionally defined as the respiratory afferent area (Saper, 2004), and functionally would appear to have an important role in the processing and integration of diverse visceral sensory inputs that contribute to the reflex control of complex motor synergies such as swallowing, gag reflex, phonation and respiration. In other territories outside the SolI, several experimental studies showed that some afferents from the rat larynx ended within the paratrigeminal nucleus (Altschuler et al. 1989; Boucher et al. 2003; Saxon & Hopkins, 2006), but they were not conveyed by the SLN (Altschuler et al. 1989). Consequently, as we injected the SLN but not the laryngeal mucosa, our results did not show afferent endings within the paratrigeminal nucleus, reinforcing the previous statement that, in the rat, these afferents are evidently derived from the IX nerve and not the X (Altschuler et al. 1989). Concerning the spinal or the principal nuclei of the V nerve, we did not find any evidence of afferent fibres ending in these nuclei, but laryngeal projections to the spinal trigeminal nucleus have been described in hamster (Hanamori & Smith, 1986), cat (Nomura & Mizuno, 1983) and lamb (Sweazey & Bradley, 1986), as well as to the principal sensory nucleus in both cat (Nomura & Mizuno, 1983) and lamb (Sweazey & Bradley, 1986). These differences could reflect interspecies variability as these projections in the rat have not been previously described or observed in the current study (Hamilton & Norgren, 1984; Altschuler et al. 1989).

Central connections of the laryngeal nerve efferent fibres

The special visceral efferent innervation to the intrinsic laryngeal muscles originates in the Amb. As described by

Bieger & Hopkins (1987), the Amb is comprised of two major divisions: the dorsal and the external formations. The dorsal formation contains special visceral efferent motoneurons innervating the muscles of the larynx, pharynx and oesophagus (Ramón y Cajal, 1909; Lawn, 1966a,b; Kalia & Mesulam, 1980a,b; Hinrichsen & Ryan, 1981; Bieger & Hopkins, 1987). It includes three serially arranged subdivisions; the most rostral is the compact formation that projects to all levels of the oesophagus; an intermediate subdivision, the semicompact formation, which contains motoneurons for the pharyngeal constrictors and also the cricothyroid muscle; and the caudalmost subdivision, the loose formation, which projects to the intrinsic laryngeal musculature with the exception of the cricothyroid muscle. The external formation, the remaining major division, lies ventrolaterally alongside the dorsal formation and contains cardiomotor preganglionic parasympathetic cells but, occasionally, some neurons with axons in either the IX nerve or the SLN, innervating yet unidentified structures above the diaphragm (Bieger & Hopkins, 1987). In our experiments combining the SLN dextran-tracing with ChAT-IH, some neurons within the external formation were observed.

In addition to the motoneurons providing special visceral efferent innervation to the larynx, there is also a parasympathetic innervation providing a secretomotor general visceral supply to the mucous glands that line the larynx cavities (Wyke & Kirchner, 1976; McHanwell, 2008). This autonomic innervation should not be overlooked as mucous secretion is important for normal laryngeal function (Basterra et al. 1988; McHanwell, 2008; Sato & Nakashima, 2008). Our results complement those from previous authors that identified the origin of these secretomotor fibres in the 10N (Kalia & Mesulam, 1980b; Hinrichsen & Ryan, 1981; Pascual-Font et al. 2006b, 2007), and confirm that in the rat these efferents travel to the larynx along the SLN but not the RLN.

Number of neurons within the Amb

Previous quantitative data on the number of neurons in the Amb projecting via the SLN in the rat showed a wide numerical range. Our results (average 119 ± 36, $n = 20$) are in the range of the previously reported population of 170 neurons within the whole semicompact formation (Bieger & Hopkins, 1987) and with the 111 ± 62 cells ($n = 10$) described in a preliminary dextran labelling study (Pascual-Font et al. 2006b). Higher numbers were reported showing totals of 197 and 276 neurons in two experiments, being HRP spreading a potential complicating factor (Hinrichsen & Ryan, 1981). Also, using HRP as a marker, an average of 71 labelled neurons was reported, this being much lower than our data but consistent with the shorter length of the Amb column for SLN neurons observed (Patrickson et al. 1991a). Finally, the reported existence of only nine labelled neurons seems unaccountably low (Furusawa et al. 1996).

With regard to the number of neurons labelled in the RLN, the average obtained in our experiments (155 ± 30, $n = 25$) is within the reported range of the 140 neurons reported for the whole loose formation (Bieger & Hopkins, 1987), the data of 163 ± 51 ($n = 9$) neurons from an earlier publication (Hinrichsen & Ryan, 1981) and the 152 ± 33 ($n = 7$) obtained in a preliminary dextran labelling study (Pascual-Font et al. 2006a).

It is always difficult to be certain how much reliance can be placed upon quantitative results obtained from tracing experiments. However, from the comparisons made above and from preliminary data obtained from retrograde mapping of individual muscle motor nuclei, we feel confident that our results are reliable. The other issue that arises in quantitative analysis is the matter of double counting. The relatively close correlation between our data gathered from counting neurons with nucleoli in nuclei labelled with DAPI and bright-field counts suggests that the relatively small errors that would be theoretically predicted, taking into account the size of the nucleolus relative to the employed section thickness, seem to be negligible in practice.

Ipsilateral vs. bilateral innervation

A number of early studies reported that, in the rat, Amb motoneurons project bilaterally to the larynx via rat laryngeal nerves (Wetzel et al. 1980; Lobera et al. 1981; Pásaro et al. 1981), leading to the suggestion that rodents retain an archaic bilateral system of laryngeal innervation compared with the more evolved ipsilateral projections seen in carnivores (Lobera et al. 1981). Subsequent studies together with the current report were unable to replicate these findings (Hinrichsen & Ryan, 1981; Bieger & Hopkins, 1987; Patrickson et al. 1991a; Furusawa et al. 1996; Pascual-Font et al. 2006a,b, 2007). The most likely explanation for the earlier findings would be that spurious labelling of the contralateral laryngeal nerve fibres occurred due to uncontrolled diffusion of HRP (Hinrichsen & Ryan, 1981; Bieger & Hopkins, 1987; Patrickson et al. 1991a; Furusawa et al. 1996).

Localisation of the neuronal columns within the Amb

Motoneurons within the Amb project to a large number of peripheral targets including the larynx, pharynx and oesophagus via some peripheral nerves and so it is not surprising, given the lack of comprehensive studies, that there is no agreement on the detailed topographical arrangement of neurons in this nucleus.

In the rat, the SLN would appear to innervate, in addition to the cricothyroid muscle, the inferior constrictor muscle (thyropharyngeus), it sends also branches to the oesophagus (some presumably muscular), and it also seems likely that it innervates some of the smaller muscles of the laryngeal inlet (Neuhuber et al. 2006; McHanwell, 2008).

The RLN supplies the other intrinsic muscles of the larynx, but it also sends branches to the oesophagus and may also innervate the inferior pharyngeal constrictor muscle (Neuhuber et al. 2006; McHanwell, 2008). In addition, and via other nerves, motoneurons within the Amb also innervate other muscles in the pharynx and palate (McHanwell, 2008).

The findings of the present study reveal that motoneurons projecting via the SLN and the RLN form a continuous column within the Amb. Taking the obex as reference (Hamilton & Norgren, 1984), we find SLN motoneurons extending rostrocaudally between 2590 and 1230 μm within the AmbSC, and RLN motoneurons extending between 1800 and −900 μm within the AmbL, thus overlapping in a territory rostral to the obex. There is general consensus that the SLN neurons are located rostrally with respect to those of the RLN and that the two populations overlap (Lawn, 1966a,b; b; Hinrichsen & Ryan, 1981; Schweizer et al. 1981; Yajima & Hayasi, 1983; Davis & Nail, 1984; Hamilton & Norgren, 1984; Bieger & Hopkins, 1987; Patrickson et al. 1991a; Furusawa et al. 1996; Pascual-Font et al. 2006a,b). However, although these studies agree in their qualitative descriptions, quantitative data are frequently omitted and, when published, reveal some conspicuous differences. Therefore, Patrickson et al. (1991a) reported neurons of the SLN located between 850 and 420 μm, and those of the RLN segregated in two subpopulations distributed between 785 and −1150 μm, and Furusawa et al. (1996) described the SLN cells disseminated between 2500 and 1500 μm. In the former report the number of labelled neurons was smaller than that counted in our study, so we consider that the most likely explanation for the discrepancies in the number and location of the neurons resides in an insufficient labelling together with an imprecise definition of the obex.

The majority of studies, including the current one, agree that motoneurons within the Amb constitute a single population of neurons located rostral to the obex (Davis & Nail, 1984; Bieger & Hopkins, 1987; Portillo & Pásaro, 1988; Patrickson et al. 1991a; Furusawa et al. 1996; Pascual-Font et al. 2006b). However, it has been stated that SLN neurons within the Amb are organised in two subpopulations, one rostral and one caudal to the obex (Hinrichsen & Ryan, 1981), or that motoneurons innervating the cricothyroid muscle are organised into two clusters (Gacek, 1975). The most likely explanation for these discrepant findings would appear to be the spread of tracer to muscles innervated by the RLN. This is supported by the fact that labelling the cricothyroid muscle without severing the RLN produced two groups of traced motoneurons (one rostral and one caudal), whereas when the ipsilateral RLN was cut prior to muscle injection, only the rostral group of cells was traced, thus concluding that the caudalmost neurons projected via the RLN (Davis & Nail, 1984).

Similar discrepancies have been reported in relation to the organisation of the RLN motoneurons within the Amb, some researchers reporting two populations of motoneurons (Hinrichsen & Ryan, 1981; Patrickson et al. 1991a). As discussed above, these results are most probably due to an undesirable spread of tracer to neighbour structures.

The functional meaning of the topographical organization of the Amb remains a matter for speculation, but it is clear that the control of the laryngeal breathing cycles, phonation process and reflexes require an exquisite central and peripheral coordination (Wyke & Kirchner, 1976; Sasaki, 2006; McHanwell, 2008). So, this rostrocaudal overlapping neuronal arrangement could reflect the anatomical substrate for that coordination, as previously suggested (Wetzel et al. 1980; Hinrichsen & Ryan, 1981; Davis & Nail, 1984; Bieger & Hopkins, 1987; Patrickson et al. 1991a).

Neurons within the dorsal nucleus of the vagus

Labelled neurons were observed in the 10N when the tracer was applied to the SLN, but never when it was applied to the RLN. There have been several studies reporting similar findings following SLN tracing (Hinrichsen & Ryan, 1981; Hamilton & Norgren, 1984; Krammer et al. 1986; Patrickson et al. 1991a; Furusawa et al. 1996; Pascual-Font et al. 2006b). When analysing the data obtained with HRP labelling of the RLN, some discrepancies appear, as only one study described that lack of labelled neurons in the 10N (Hinrichsen & Ryan, 1981), whereas others reported labelled motoneurons in the 10N (Wetzel et al. 1980; Patrickson et al. 1991a), the above-mentioned technical issues related to HRP probably being the origin of these differences.

The most probable function of the laryngeal neurons of the 10N is to provide preganglionic parasympathetic secretomotor innervation to the submucous glands of the larynx (Hinrichsen & Ryan, 1981; Hamilton & Norgren, 1984; Patrickson et al. 1991a). This innervation is essential for the normal laryngeal physiology, providing mucous secretion to protect the vocal folds and to reduce resistance to airflow (Basterra et al. 1988; McHanwell, 2008; Sato & Nakashima, 2008).

In our experiments, the mean number of labelled neurons was 75 ± 25 (n = 19), similar to an earlier study reporting 69 (Patrickson et al. 1991a). Another study has reported a slightly lower number of 41 (n = 5; Furusawa et al. 1996). An earlier study found 188 labelled neurons (n = 2; Hinrichsen & Ryan, 1981), but this high number is probably due to the HRP spreading to the adjacent oesophagus. Furthermore, as the total number of experiments in our study is larger than the previously reported ones, the number of neurons observed is probably more accurate with potential errors due to interindividual variability decreased.

The distribution found for these neurons, found rostral to the obex from 1390 to 2700 μm, was similar to the previously published data (Furusawa et al. 1996).

Conclusions

The results of our study present a comprehensive analysis of the central projections of the adult rat laryngeal nerves using a reliable neuronal tracer applied directly to the cut nerves. The report clarifies some of the unresolved discrepancies in the published literature concerning the central origin of the fibres of the laryngeal nerves, and serves to establish a model for future studies on the neuronal reorganisation of the Amb after the injury of laryngeal nerves.

The main conclusions of the study are as follows.

– The central projections of the laryngeal nerves are exclusively ipsilateral.

– The SLN has special visceral efferent, general visceral efferent and general visceral afferent fibres projecting from the Amb, the dorsal motor nucleus of the vagus and to the Sol, respectively.

– The RLN contains exclusively special visceral efferent fibres projecting from the Amb.

– The motoneurons of the SLN are located rostral to the motoneurons of the RLN within the Amb, but both populations overlap in a region of the nucleus located rostrally to the obex.

Acknowledgements

References

Altschuler SM, Bao XM, Bieger D, et al. (1989) Viscerotopic representation of the upper alimentary tract in the rat: sensory ganglia and nuclei of the solitary and spinal trigeminal tracts. *J Comp Neurol* **283**, 248–268.

Basterra J, Chumbley CC, Dilly PN (1988) The superior laryngeal nerve: its projection to the dorsal motor nucleus of the vagus in the guinea pig. *Laryngoscope* **98**, 89–92.

Berke GS, Ye M, Block RM, et al. (1993) Orthotopic laryngeal transplantation: it is time? *Laryngoscope* **103**, 857–864.

Bieger D, Hopkins DA (1987) Viscerotopic representation of the upper alimentary tract in the medulla oblongata in the rat: the nucleus ambiguus. *J Comp Neurol* **262**, 546–562.

Boucher Y, Simons CT, Cuellar JM, et al. (2003) Activation of brain stem neurons by irritant chemical stimulation of the throat assessed by c-fos immunohistochemistry. *Exp Brain Res* **148**, 211–218.

Brondbo K, Jacobsen E, Gjellan M, et al. (1992) Recurrent nerve ⁄ ansa cervicalis nerve anastomosis: a treatment alternative in unilateral recurrent nerve paralysis. *Acta Otolaryngol* **112**, 353–357.

Crumley RL (1982) Experiments in laryngeal reinnervation. *Laryngoscope* **92**(9 Pt 2 Suppl 30), 1–27.

Crumley RL (2000) Laryngeal synkinesis revisited. *Ann Otol Rhinol Laryngol* **109**, 365–371.

Davis PJ, Nail BS (1984) On the location and size of laryngeal motoneurons in the cat and rabbit. *J Comp Neurol* **20**, 13–32.

Fritzsch B (1993) Fast axonal diffusion of 3000 molecular weight dextran amines. *J Neurosci Meth* **50**, 95–103.

Furusawa K, Yasuda K, Okuda D, et al. (1996) Central distribution and peripheral functional properties of afferent and efferent components of the superior laryngeal nerve: morphological and electrophysiological studies in the rat. *J Comp Neurol* **375**, 147–156.

Gacek RR (1975) Localization of laryngeal motor neurons in the kitten. *Laryngoscope* **85**, 1841–1861.

Glover JC, Petursdottir G, Jansen JK (1986) Fluorescent dextran-amines used as neuronal tracers in the nervous system of the chicken embryo. *J Neurosci Meth* **18**, 243–254.

Hamilton RB, Norgren R (1984) Central projections of gustatory nerves in the rat. *J Comp Neurol* **222**, 560–577.

Hanamori T, Smith DV (1986) Central projections of the hamster superior laryngeal nerve. *Brain Res Bull* **16**, 271–279.

Hinrichsen CFL, Ryan T (1981) Localization of laryngeal motoneurons in the rat: morphologic evidence for dual innervation? *Exp Neurol* **74**, 341–355.

Hisa Y, Lyon MJ, Malmgren LT (1985) Central projection of the sensory component of the rat recurrent laryngeal nerve. *Neurosci Lett* **5**, 185–190.

Kalia M, Mesulam MM (1980a) Brainstem projections of sensory and motor components of the vagus complex in the cat: I. The cervical vagus and nodose ganglion. *J Comp Neurol* **193**, 435–465.

Kalia M, Mesulam MM (1980b) Brainstem projections of sensory and motor components of the vagus complex in the cat: II. Laryngeal, tracheobronchial, pulmonary, cardiac and gastrointestinal branches. *J Comp Neurol* **193**, 467–508.

Kalia M, Richter D (1985) Morphology of physiologically identified slowly adapting lung stretch receptor afferents stained with intra-axonal horseradish peroxidase in the nucleus of the tractus solitarius of the cat. I. A light microscopic analysis. *J Comp Neurol* **241**, 503–520.

Kalia M, Richter D (1988) Rapidly adapting pulmonary receptor afferents: I. Arborization in the nucleus of the tractus solitarius. *J Comp Neurol* **274**, 560–573.

Krammer EB, Streinzer W, Millesi W, et al. (1986) Zentrale lokalisation motorischer komponenten im ramus internus des m. laryngeus superior: eine HRP-studie bei der ratte. *Laryngol Rhinol Otol* **65**, 617–620.

Lawn AM (1966a) The localization, in the nucleus ambiguus of the rabbit, of the cells of origin of motor nerve fibers in the glossopharyngeal nerve and various branches of the vagus nerve by means of retrograde degeneration. *J Comp Neurol* **127**, 293–306.

Lawn AM (1966b) The nucleus ambiguus of the rabbit. *J Comp Neurol* **127**, 307–320.

Lobera B, Pásaro R, González-Barón S, et al. (1981) A morphological study of ambiguus nucleus motoneurons innervating the laryngeal muscles in the rat and cat. *Neurosci Lett* **23**, 125–130.

López JM, Morona R, Moreno N, et al. (2007) Origins of spinal cholinergic pathways in amphibians demonstrated by retrograde transport and choline acetyltransferase immunohistochemistry. *Neurosci Lett* **425**, 733–737.

Maranillo E, Leon X, Quer M, et al. (2003) Is the external laryngeal nerve an exclusively motor nerve? The cricothyroid connection branch. *Laryngoscope* **113**, 525–529.

Marín O, González A (1999) Origin of tectal cholinergic projections in amphibians: a combiner study of choline acetyl transferase immunohistochemistry and retrograde transport of dextran amines. *Vis Neurosci* **16**, 271–283.

McHanwell S (2008) The larynx. In: *Gray's Anatomy 40th*. (ed. Standring S), pp. 577–594. London: Churchill Livingstone.

McHanwell S, Biscoe TJ (1981a) The localization of motoneurons supplying the hindlimb of the mouse. *Philos Trans R Soc Lond B* **293**, 477–508.

McHanwell S, Biscoe TJ (1981b) The sizes of motoneurons supplying the hindlimb of the mouse. *Proc R Soc Lond B* **213**, 201–216.

Moore KL, Dalley AF (2006) *Clinically Oriented Anatomy*, 5th edn. Baltimore: Lippincott Williams & Wilkins.

Morrison MD (1952) Recurrent laryngeal nerve paralysis. A revised conception based on the dissection of one hundred cadavers. *Ann Otol Rhinol Laryngol* **61**, 567–592.

Nasri S, Beizai P, Ye YM, et al. (1997) Cross-innervation of the thyroarytenoid muscle by a branch from the external division of the superior laryngeal nerve. *Ann Otol Rhinol Laryngol* **106**, 594–598.

Neuhuber WL, Raab M, Bethoud HR, et al. (2006) Innervation of the mammalian esophagus. *Adv Anat Embryol Cell Biol* **185**, 1–73.

Nomura S, Mizuno N (1983) Central distribution of efferent and afferent components of the cervical branches of the vagus nerve. A HRP study in the cat. *Anat Embryol* **166**, 1–18.

Ogura J.H., Harvey JE, Mogi G (1970) Further experimental observations of transplantation of canine larynx. *Laryngoscope* **80**, 1231–1243.

Pásaro R, Lobera B, González-Barón S, et al. (1981) Localización de las motoneuronas de los músculos intrínsecos de la laringe de la rata. *Rev Esp Fisiol* **37**, 317–322.

Pásaro R, Lobera S, González-Barón S, et al. (1983) Cytoarchitectonic organization of laryngeal motoneurons within the nucleus ambiguus of the cat. *Exp Neurol* **82**, 623–634.

Pascual-Font A, Maranillo E, Merchán A, et al. (2006a) Central projections of the rat recurrent laryngeal nerve. *Acta Otorrinolaringol Esp* **57**, 253–256.

Pascual-Font A, Maranillo E, Merchán A, et al. (2006b) Central projections of the rat superior laryngeal nerve. *Acta Otorrinolaringol Esp* **57**, 295–299.

Pascual-Font A, Maranillo E, Merchán A, et al. (2006c) Morphometry of the recurrent laryngeal nerve of the rat. *Acta Otorrinolaringol Esp* **57**, 435–440.

Pascual-Font A, Maranillo E, Merchán A, et al. (2007) Dogmas in anatomy and neuroanatomy: the central projections of the rat's recurrent and superior laryngeal nerves. *J Anat* **210**, 606.

Patrickson JW, Smith TE, Zhou JW (1991a) Motor neurons of the laryngeal nerves. *Anat Rec* **230**, 551–556.

Patrickson JW, Smith TE, Zhou JW (1991b) Afferent projections of the superior and recurrent laryngeal nerves. *Brain Res* **539**, 169–174.

Paxinos G, Watson C (2005) *The Rat Brain in Stereotaxic Coordinates*, 5th edn. London: Elsevier Academic Press.

Popov S, Poo MM (1992) Diffusional transport of macromolecules in developing nerve processes. *J Neurosci* **12**, 77–85.

Portillo F, Pásaro R (1988) Location of motoneurons supplying the intrinsic laryngeal muscles of rats. Horseradish peroxidase and fluorescence double-labelling study. *Brain Behav Evol* **32**, 220–225.

Ramón y Cajal S (1909) *Histologie du Système Nerveux de l'homme et des vertébrés*. Paris: Malaine.

Ranson RN, Butler PJ, Taylor EW (1995) Studies on nerves of the upper respiratory tract in the ferret and the mink. *J Auton Nerv Syst* **52**, 1–16.

Reiner A, Veenman CL, Medina L, et al. (2000) Pathway tracing using biotinylated dextran amines. *J Neurosci Meth* **103**, 23–37.

Sánchez-Camacho C, Peña JJ, González A (2003) Catecholaminergic innervation of the septum in the frog: a combined immunohistochemical and tract-tracing study. *J Comp Neurol* **455**, 310–323.

Sánchez-Camacho C, Peña JJ, González A (2006) Basal forebrain cholinergic system of the anuran amphibian Rana perezi: evidence for a shared organization pattern with amniotes. *J Comp Neurol* **494**, 961–975.

Sañudo JR, Maranillo E, Leon X, et al. (1999) An anatomical study of anastomoses between the laryngeal nerves. *Laryngoscope* **109**, 983–987.

Saper CB (2004) Central autonomic system. In: *The Rat Nervous System*, 3rd edn. (ed. Paxinos G), pp. 761–784. London: Elsevier.

Sasaki CT (2006) Anatomy and development and physiology of the larynx. [Online]. Raj Goyal and Reza Shaker: GI Motility online. Available at: http://www.nature.com/gimo/contents/pt1/full/gimo7.html [Accessed 19 December 2007].

Sato K, Nakashima T (2008) Effect of irradiation on the human laryngeal glands. *Ann Otol Rhinol Laryngol* **117**, 734–739.

Saxon DW, Hopkins DA (2006) Ultrastructure and synaptology of the paratrigeminal nucleus in the rat: primary pharyngeal and laryngeal afferent projections. *Synapse* **15**, 220–234.

Schweizer H, Ruebsamen R, Ruehle C (1981) Localization of brain stem motoneurons innervating the laryngeal muscles in the rufous horseshoe bat. *Brain Res* **230**, 41–50.

Suzuki M, Kirchner JA (1968) Afferent nerve fibers in the external branch of the superior laryngeal nerve in cat. *Ann Otol Rhinol Laryngol* **77**, 1059–1070.

Sweazey RD, Bradley RM (1986) Central connections of the lingual-tonsillar branch of the glossopharyngeal nerve and the superior laryngeal nerve in lamb. *J Comp Neurol* **245**, 471–482.

Szentágothai J (1943) Die Lokalisation der Kehlkopfmuskulatur in den Vaguskernen. *Z Anat Ent- wicklungsgesch* **112**, 704–710.

Wank M, Neuhuber WL (2001) Local differences in vagal afferent innervation of the rat esophagus are reflected by neurochemical differences at the level of the sensory ganglia and by different brainstem projections. *J Comp Neurol* **435**, 41–59.

Wetzel DM, Kelley DB, Campbell BA (1980) Central control of ultrasonic vocalizations in neonatal rats: I. Brain stem motor nuclei. *J Comp Physiol Psychol* **94**, 596–605.

Wyke BD, Kirchner JA (1976) Neurology of the larynx. In: *Scientific Foundations of Otolaryngology*. (eds Hinchciffe R, Harrison D), pp. 546–574. London: William Heinneman Medical Books.

Yajima Y, Hayasi Y (1983) Identification of motoneurons in the nucleus ambiguus by antidromic stimulation of the superior and the recurrent laryngeal nerves in rats. *Brain Res* **288**, 302–306.

Yoshida Y, Miyazaki T, Hirano M, et al. (1982) Arrangement of motoneurons innervating the intrinsic laryngeal muscles of cats as demonstrated by horseradish peroxidase. *Acta Otolaryngol* **94**, 329–334.

Zheng H, Li Z, Zhou S, et al. (1996) Laryngeal reinnervation for unilateral vocal cord paralysis with the ansa cervicalis. *Laryngoscope* **106**, 1522–1527.